International Journal of Chemistry; Vol. 16, No. 1; 2024
ISSN 1916-9698 E-ISSN 1916-9701
Published by Canadian Center of Science and Education

Elaborating the Link Between VSEPR and Orbital Hybridization

Allan R. Pinhas[1], Roger W. Kugel[1], William B. Jensen[1]

[1]Department of Chemistry, University of Cincinnati, Cincinnati, OH 45221-0172, USA

Correspondence: Allan R. Pinhas, Department of Chemistry, University of Cincinnati, Cincinnati, OH 45221-0172, USA.

Received: January 15, 2024 Accepted: February 26, 2024 Online Published: February 29, 2024

doi:10.5539/ijc.v16n1p57 URL: https://doi.org/10.5539/ijc.v16n1p57

Abstract

Many undergraduate chemistry textbooks discuss both the VSEPR (valence-shell electron-pair repulsion) and hybridization (the mixing of atomic orbitals to form new directional orbitals) models of molecular structure as separate topics and fail to mention Bent's rule (the more electronegative ligand uses the hybrid bonding orbital with the greatest *p*-character). In this paper, important, but neglected, correlations among these three topics are explored. In addition, it is shown how a consideration of these correlations makes each of the topics more understandable to students.

Keywords: bond angle, hybridization, VSEPR, Bent's Rule, electronegativity, acidity

1. Introduction

As is taught in general chemistry courses, the H-C-H bond angle of methane (CH_4) is 109.5º, the H-N-H bond angle of ammonia (NH_3) is 107.3º, and the H-O-H bond angle of water (H_2O) is 104.5º. This paper deals with molecules of the general formula AX_nE_m, in which A is a central atom, X is a ligand bonded to the central atom, E is a lone pair of electrons, and $n + m = 4$. The major focus of this paper is the question of why these angles are different. Initially, VSEPR, hybridization, and Bent's rule will be discussed, followed by some neglected correlations among these three topics, which will make each of them easier for students to understand. In the Appendix, we present several examples of the correlations between bond angles, percent *p*-character in the bonding orbitals, and the electronegativity difference of the bonded atoms.

2. The VSEPR Model

Discussions of the valence-shell electron-pair repulsion or VSEPR model of molecular geometry are now found in virtually all introductory chemistry textbooks (Brown, LeMay et al., 2022; Moore & Stanitski, 2015; Silberberg & Amateis, 2021), and in many undergraduate inorganic and organic textbooks as well (Holleman & Wiberg, 2001; MacKay & Henderson, 2017; Miessler & Tarr, 2011; Brown, Iverson, et al., 2023; Karty, 2018; Klein, 2021; Loudon & Parise, 2021; Mullins, 2021; Wade & Simek, 2017). First proposed by Gillespie and Nyholm in 1957, this model can be formulated as a series of simple rules, the most important of which is the premise that (Gillespie & Nyholm, 1957):

(Rule 1): *Molecular geometry is the result of having minimized the repulsions between the electron pairs, both bonding and nonbonding, found in the valence shell of the central atom of a discrete molecule or complex ion*.

Although many textbook accounts of the model fail to explain the origins of these repulsions, it was originally suggested by Gillespie that they are the combined result of both electrostatic repulsion and the operation of the Pauli exclusion principle. Given a simple molecule of composition AX_nE_m, where A is the central atom, n is the number of ligands (X) or bonding electron pairs, and m is the number of lone electron pairs (E) in the valence shell of A, Rule 1 successfully predicts, for the case in which there are no lone pairs present (i.e., $m = 0$), all of the basic coordination polyhedra found for simple molecules. Introductory textbooks usually report these results for n = 1-6 ligands, whereas specialty monographs give the results for n = 1-9 ligands (Gillespie, 1972; Gillespie & Hargittai, 1991; Kepert, 1982).

In the case where one or more lone pairs are present (i.e., $m \geq 1$), the model also successfully predicts that the resulting molecular structures will correspond to fragments of these complete polyhedra in which one or more of the vertices has been replaced by a lone pair. Thus, the pyramidal structure of NH_3, which is an AX_3E molecule with a total of four electron pairs in the valence shell of N, is viewed as a fragment of a tetrahedron in which one of the vertices is occupied by a lone pair. Likewise, the bent structure of H_2O, which is a AX_2E_2 molecule, also with a total of four electron pairs in the valence shell of O, is similarly viewed as a fragment of a tetrahedron in which two of the vertices have been replaced by two lone pairs. However, the resulting X-A-X bond angles in both NH_3 (107.3º) and H_2O (104.5º) deviate

slightly from those (109.5º) found for a true tetrahedral AX_4 molecule like CH_4, with no lone pairs. VSEPR rationalizes these distortions using the rule that the lone pairs (LP) exert a greater repulsion than the bonding pairs (BP), thus giving rise to the following repulsion sequence:

(Rule 2): $$LP\text{-}LP > LP\text{-}BP > BP\text{-}BP \quad (1)$$

Hence, because NH_3 has only one lone pair, its deviation from the ideal angles of a perfect tetrahedron is not as great as those for H_2O, with two lone pairs. Many introductory textbooks simply state Rule 2 as a given. The few textbooks that offer an underlying theoretical rationale, point out that bonding pairs are under the electrostatic influence of two positively charged atomic cores (those of the central atom and the bound ligand), whereas lone pairs are under the influence of only one (that of the central atom) (Gillespie et al., 1986). This causes the bonding pairs to contract more than the lone pairs and so occupy less angular spread in the valence shell of the central atom.

Seldom mentioned in introductory textbook accounts of VSEPR is the further rule that:

(Rule 3): *The more electronegative a ligand, the greater the contraction of its corresponding bonding pair and the smaller its repulsion and angular spread relative to any other electron pairs that happen to be present in the valence shell of the central atom* (Gillespie, 1972).

Thus, despite the fact that both phosphorous trifluoride and phosphorus triiodide have the same basic AX_3E geometry, with only one lone pair, the bond angles in the former (97.8°) are significantly smaller than those in the latter (102°), in keeping with the fact that fluorine is more electronegative than iodine.

3. The Hybridization Model

The second approach to molecular geometry discussed in most introductory chemistry textbooks is the orbital hybridization model introduced independently by both Pauling and Slater in 1931 within the context of valence bond (VB) theory (Pauling, 1931; Slater, 1931). This model postulates that the energy required to hybridize the ground-state atomic orbitals of the central atom of a simple molecule or complex ion, in order to create directional bonds, is driven by the necessity of maximizing the orbital overlap between the orbitals of the central atom and those of the bound ligands, so as to form the strongest possible A-X bonds. Unfortunately, many introductory textbooks do not mention this theoretical rationale for orbital hybridization. Consequently, the resulting hybrid orbitals are presented as little more than after-the-fact memorized labels (e.g., *sp*, sp^2, sp^3 etc.) for each basic molecular shape or polyhedron. Since, for a given hybridization scheme, the resulting orbitals are all represented as being equivalent (i.e., the same shape and size), no rationale is offered for any deviations from the corresponding idealized bond angles when lone pairs are present. Even more serious is the fact that the degree of overlap between two interacting orbitals must be calculated using quantum mechanics, and this means that, unlike the VSEPR model, the hybridization model cannot be used to qualitatively predict geometry at the introductory level (However, it is possible to work backwards and calculate the degree of hybridization from the known bond angles.) Because of these limitations, some chemical educators have advocated the removal of the hybridization model from the introductory textbook (Grushow, 2011).

4. Connecting the Two Models

To the extent that introductory textbooks connect the two models, the valence electron pairs of the Lewis diagram for the molecule or complex ions are each assigned to a hybrid orbital and, in keeping with the VSEPR rule 2 that lone pairs occupy more space than bonding pairs, it is further assumed that the hybrid orbitals for the former are larger than those for the latter. Thus, the repulsions between the various electron pairs are no longer pictured in terms of repulsions between point charges, but rather in terms of repulsions between the electron clouds of each hybridized orbital. But how do the resulting labels for the required change in the size of the hybrid orbitals for lone pairs reflect this size change and hence the resulting deviations from the idealized polyhedral angles?

The answer lies in the realization that the degree of orbital hybridization does not necessarily have to result in only integral numerical superscripts in the corresponding orbital labels. Rather, the ratio in which the component atomic orbitals are mixed may be varied continuously, and thus result in fractional values as well. In the case of a central atom using only its *s* and *p* atomic orbitals for hybridization, the hybridization index (*i*) for the resulting sp^i hybrid is defined as the fraction (or percentage) of the *p*-orbital (f_p) used in forming a hybridized atomic orbital divided by the fraction (or percentage) of the *s*-orbital (f_s) used (Hsu & Orchin, 1972; Huheey, Keiter, & Keiter, 1993):

$$i = f_p/f_s \quad (2)$$

For example, for an *sp*-hybrid orbital, which is 50% *p* and 50% *s*, $i = 0.5/0.5 = 1$: for an sp^2-hybrid orbital, which is 66.67% *p* and 33.33% *s*, $i = 0.6667/0.3333 = 2$; and for an sp^3-hybrid orbital, which is 75% *p* and 25% *s*, $i = 0.75/0.25 = 3$. In general, the larger *i*, the larger the *p*-orbital contribution to the hybrid and the smaller *i*, the larger the *s*-orbital contribution to the hybrid. Thus, an sp^2-hybrid orbital has greater *s*-character (or less *p*-character) than an sp^3-hybrid

orbital. In keeping with equation 2, this also means that, contrary to popular belief, *i does not necessarily represent the number of p-orbitals used to create the hybrid* and therefore may assume not only fractional values but values greater than three.

For each individual hybrid orbital, the contributing *s*-fraction and *p*-fraction must sum to 1:

$$f_s + f_p = 1 \tag{3}$$

Consequently, if there is a total of *n* hybrid orbitals around a central atom, the sum of the *s* and *p* contributions must be equal to *n*:

$$\Sigma f_s + \Sigma f_p = n \tag{4}$$

In equation 4, the first term is equal to 1, because there is only one *s*-orbital available on the central atom:

$$\Sigma f_s = 1 \tag{5}$$

and thus, it follows that the second term must equal *n*-1:

$$\Sigma f_p = n - 1 \tag{6}$$

where *n*-1 is equal to 1, 2, or 3, depending on how many of the three *p*-orbitals on the central atom are used for hybrid orbital formation. Solving equation 2 for f_s or f_p and substituting into equation 3 then allows f_s and f_p for a given hybrid orbital to be expressed as a function of *i*:

$$f_s = 1 / (1 + i) \tag{7}$$

$$f_p = i / (1 + i) \tag{8}$$

As stated above, the single most common misconception about hybridization found in the introductory textbook is that $(n - 1) = i$, in other words, that *i* must be a whole number. *In actual fact, the relation (n – 1) = i is true only if the n hybrid orbitals around the central atom are all equivalent.* However, nothing in the hybridization process requires them to be equivalent, and thus, nothing requires that the *i* value must necessarily be an integer.

As shown in Figure 1, a direct plot of the X-A-X bond angle θ vs. f_p/f_s, or *i* gives a curve for the case of the three standard *sp*, sp^2 and sp^3 hybrid orbitals:

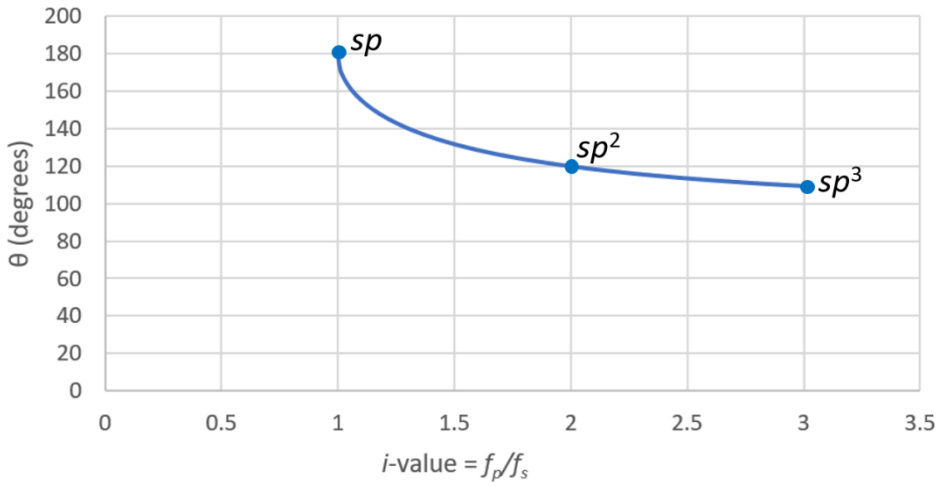

Figure 1. Plot of bond angle vs. *i* value for sp^3, sp^2, and *sp* hybrid orbitals

As shown in Figure 2, this may be transformed into a straight-line using the following equation (Hsu & Orchin, 1972; Huheey, Keiter, & Keiter, 1993):

$$-\cos\theta = 1 / i = f_s / f_p \tag{9}$$

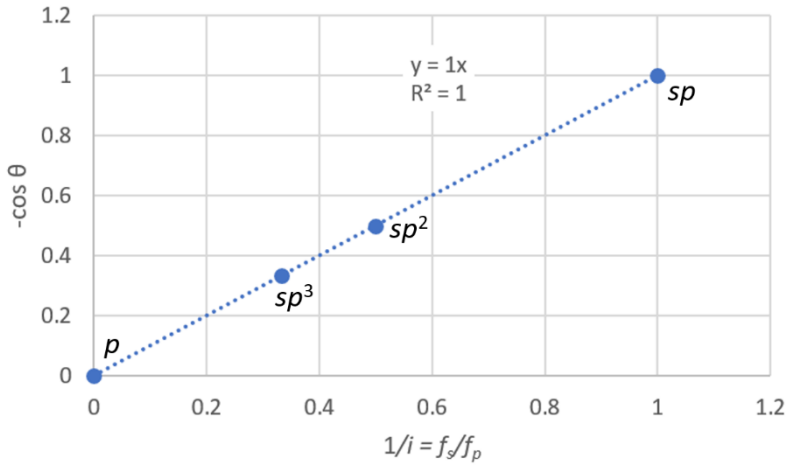

Figure 2. Plot of –cos θ versus 1/*i* for pure *p* and sp^3, sp^2, and *sp* hybrid orbitals (Note that $f_s/f_p = 0$ for a pure *p* orbital since, in that case, $f_s = 0$.)

Using equation 9, one can easily calculate *i*, if θ is known, and vice versa. Thus, for example, substituting the observed H-N-H bond angle of 107.3º for NH_3 gives $i = 3.36$ for each of the hybrid orbitals on nitrogen pointing to a hydrogen. Put another way, each of the three N-H bonding orbitals on ammonia is generated from an *s* orbital on hydrogen and an $sp^{3.36}$-hybrid orbital on nitrogen. Using Equations 7 and 8 gives f_s (N-H) = 0.229 and f_p (N-H) = 0.771. Substituting these values into Equation 5 to get the *s*-orbital fraction in the lone pair, and into equation 3 to get the *p*-orbital fraction in the lone pair, gives f_s (lone pair) = 0.313 and f_p (lone pair) = 1 - 0.313 = 0.687. Thus, for the lone pair on the nitrogen atom, i = 0.687/0.313 = 2.19, i.e., the lone pair of electrons on the nitrogen atom of ammonia occupies a $sp^{2.19}$-hybrid orbital. These results are summarized in Table 1. Using its observed bond angle of 104.5º, a similar set of calculations can be done for water, the results of which are also shown in Table 1.

Table 1. Calculated values of *i*, f_s, f_p and the degree of hybridization, sp^i, for NH_3 and H_2O

	i	f_s	f_p	sp^i
N-H bonding pairs	3.36	0.229	0.771	$sp^{3.36}$
NH_3 lone pair	2.19	0.313	0.687	$sp^{2.19}$
O-H bonding pairs	3.99	0.200	0.800	$sp^{3.99}$
H_2O lone pairs	2.33	0.300	0.700	$sp^{2.33}$

Note that, for both NH_3 and H_2O, these results show that the lone pair hybrids contain more *s*-character than do the bonding hybrids. Pure unhybridized *p*-orbitals obviously have less angular spread than does a pure *s*-orbital. This means that the hybrids for the lone pairs in both molecules occupy more angular space or spread than the bonding orbitals, as required by Rule 2 of the VESPR model.

5. Bent's Rule

But how are we to further rationalize, using hybrid orbitals, Rule 3 of the VSEPR model? This requires that the more electronegative a ligand, the greater the contraction of the corresponding bonding pair and the smaller its repulsion and angular spread relative to any other electron pairs that happen to be present in the valence shell of the central atom. Here we can invoke a qualitative rule first formulated by Bent in the 1960s (Bent, 1960 and 1961). This rule states that the greater electronegativity difference between a ligand and the central atom, the greater the *p*-character used in the hybridized orbital for their bond and the less its angular spread in the central atom's valence shell. Thus, for a sequence of AX_3E molecules in which A is held constant but X is varied, we obtain the results in Table 2 and Figure 3. In Table 2, $\Delta EN = EN_X - EN_A$ is the electronegativity difference between A and X on the Pauling scale (Pauling, 1960) and f_p is the *p*-character of the bonding pairs calculated from the experimental bond angles. As predicted by Bent's rule, f_p obviously increases as the value of ΔEN increases across the sequence, while the bond angles simultaneously decrease. Also note that as f_p increases for the bonding orbitals, it must decrease for the lone pair.

Table 2. Variation in f_p for an AX_3E sequence in which X is varied

Molecule: AX_3E	**PI_3**	**PBr_3**	**PCl_3**	**PF_3**
X-A-X angle (degrees) [a]	102.0	101.5	100.3	97.8
$\Delta EN = EN_X - EN_A$ [b]	0.4	0.7	0.8	1.8
f_p (in the A-X bonds) [c]	0.828	0.834	0.848	0.880
f_s (in the A-X bonds) [c]	0.172	0.166	0.152	0.120
sp^i (in the A-X bonds) [c]	$sp^{4.81}$	$sp^{5.02}$	$sp^{5.59}$	$sp^{7.37}$
f_p (in the lone pair) [c]	0.516	0.499	0.455	0.358
f_s (in the lone pair) [c]	0.484	0.501	0.545	0.642

[a] Bond angles in degrees from Gillespie, 1972

[b] Values of ΔEN calculated from Pauling electronegativities.

[c] Values of i, f_p, and f_s calculated from equations 7, 8, and 9.

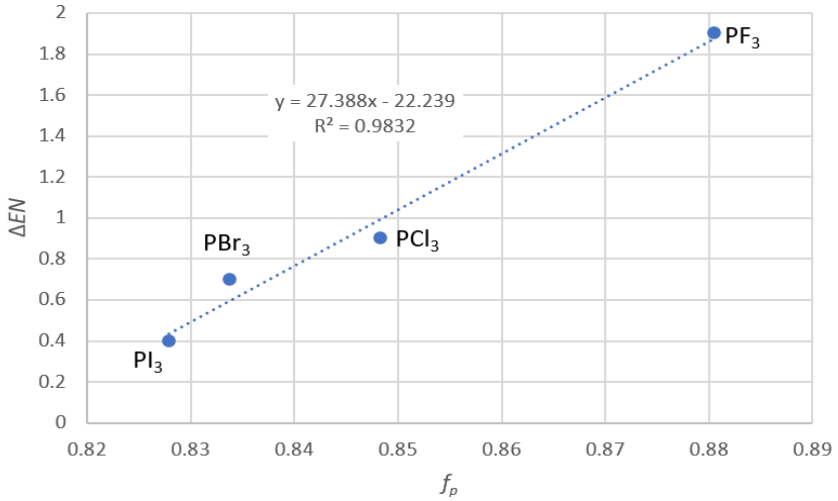

Figure 3. The linear correlation between ΔEN and f_p of the A-X bonding pair for an AX_3E sequence in which X is varied but A is held constant

A similar correlation is obtained for an AX_3E sequence in which A is varied but X is held constant as shown in Table 3 and Figure 4:

Table 3. Variation in f_p for an AX_3E sequence in which A varies but X is constant

Molecule: AX_3E	**NF_3**	**PF_3**	**AsF_3**	**SbF_3**
X-A-X angle (degrees) [a]	102.1	97.8	96.2	94.9*
$\Delta EN = EN_X - EN_A$ [b]	1.0	1.9	2.0	2.1
f_p (in the A-X bonds) [c]	0.827	0.880	0.902	0.921
f_s (in the A-X bonds) [c]	0.173	0.120	0.098	0.079
sp^i (in the A-X bonds) [c]	$sp^{4.77}$	$sp^{7.37}$	$sp^{9.26}$	$sp^{11.71}$
f_p (in the lone pair) [c]	0.520	0.358	0.292	0.236
f_s (in the lone pair) [c]	0.480	0.642	0.708	0.764

[a] Bond angles in degrees from Gillespie, 1972

[b] Values of ΔEN calculated from Pauling electronegativities.

[c] Values of i, f_p, and f_s calculated from bond angles and equations 7, 8, and 9

* Many sources report a bond angle of 88° for SbF_3. Using only *s*- and *p*-atomic orbitals, the hybridization model cannot deal with bond angles less than 90°. The angle used here was experimentally redetermined by Molnar et al. in 1997.

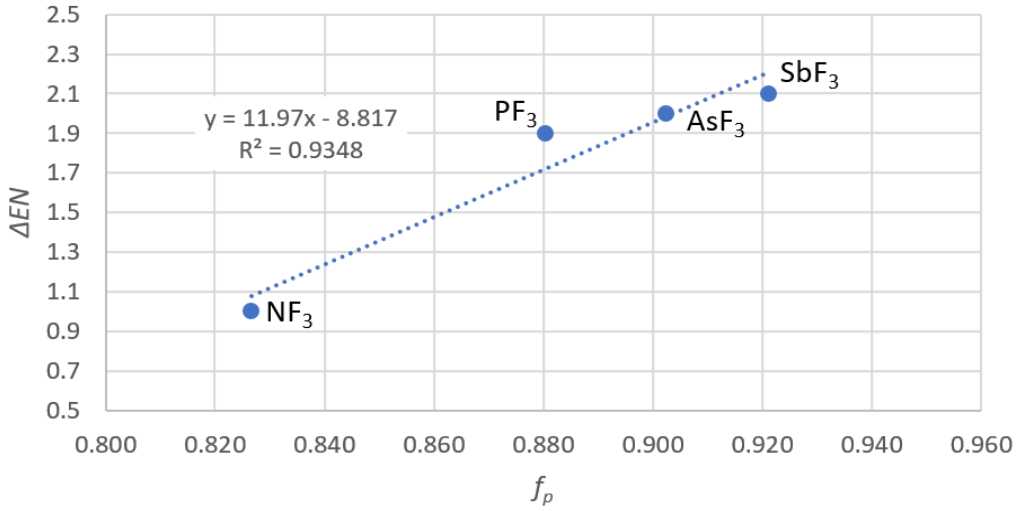

Figure 4. The linear correlation between ΔEN and f_p of the A-X bonding pair for an AX_3E sequence in which A is varied but X is held constant

Since a lone pair may be formally viewed as bonding to an imaginary ligand of zero electronegativity, Bent's rule is also consistent with Rule 2 of the VESPR model. This is illustrated by the results of the calculations in the previous section for NH_3 and H_2O, which show that the hybrid bonding orbitals in NH_3 have more *p*-character (f_p = 0.771) than does the hybrid orbital for its lone pair (f_p = 0.687), and that the two bonding pairs on O in H_2O have greater *p*-character (f_p = 0.800) than do the hybrid orbitals for its lone pairs (f_p = 0700). Additional examples of these correlations are shown in the Appendix.

6. Hydrocarbon Acidities

Weinhold and Landis in 2005 have pointed out that Bent's rule can be stated in two different, but equivalent, ways – one involving the change in the *p*-character of the bonding pairs and the other involving the change in the *s*-character of the lone pairs (Weinhold & Landis, 2005). We used the first version in the previous section in order to reflect Rule 3 of the VSEPR model. In this section we want to call attention to the second version, as originally emphasized by Bent (1960 and 1961).

It is well known that acetylene ($pK_a(C_2H_2)$ = 25) is more acidic than ethylene ($pK_a(C_2H_4)$ = 44), which in turn is more acidic than methane ($pK_a(CH_4)$ = 48), which is more acidic than ethane ($pK_a(C_2H_6)$ = 50) (March, 1992; Baldasare & Seybold, 2020). Table 4 lists these pK_a values as well as the calculated bond angles and fraction of *p*-character, f_p, in the corresponding C-H bonds for these molecules. Figure 5 shows a plot of pK_a versus f_p for these organic compounds. The resulting correlation illustrates that the acidity of C-H hybrid orbitals depends inversely on their degree of *p*-character, consistent with experimental observations and with Bent's rule. Interpreted using the second version of Bent's rule, this trend is equivalent to the presence of increasing *s*-character in the resulting lone pair of the conjugate anionic base for these molecules. This increasing *s*-character means, in turn, that the lone pair is closer to the positive core of the carbon atom in question and, as a consequence, its lone pair is a poorer electron donor – whence the increasing acidity and lower pK_a.

Table 4. Variation in f_p for the sequence: C_2H_2, C_2H_4, CH_4, C_2H_6

Molecule:	**C_2H_2**	**C_2H_4**	**CH_4**	**C_2H_6**
H-C-H angle (degrees) [a]	180.000	116.559	109.471	107.592
pK_a [b]	25	44	48	50
f_p (in the C-H bonds) [c]	0.500	0.691	0.750	0.768
f_s (in the C-H bonds) [c]	0.500	0.309	0.250	0.232
sp^i (in the C-H bonds) [c]	$sp^{1.00}$	$sp^{2.23}$	$sp^{3.00}$	$sp^{3.31}$

[a] Bond angles in degrees calculated by DFT B3LYP, 6-311G++(d,2p). Bond angle for C_2H_2 is hypothetical.

[b] Pauling, 1960

[c] Values of *i*, f_p, and f_s calculated from bond angles and equations 7, 8 and 9.

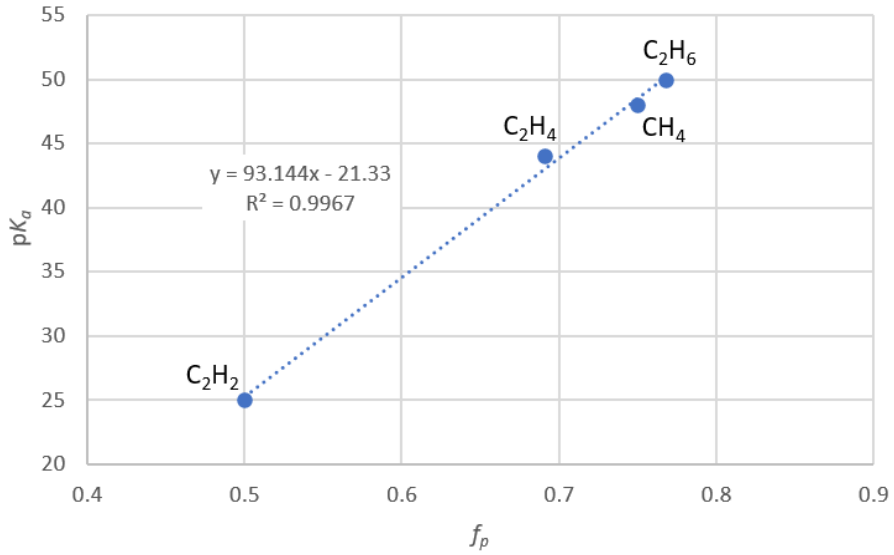

Figure 5. The pK_a of hydrocarbons vs. the fraction, f_p, of *p*-character in the C-H hybrid orbital

7. Conclusions

Within the context of the hybrid orbital representation of molecular structure, the differences in the bond angles in the sequence CH_4, NH_3, and H_2O can best be described by invoking the differences in the *s*- and *p*-characters of the hybrid orbitals used to describe the lone electron pairs versus the bonding electron pairs in these molecules. This, in turn, requires that introductory textbooks present a more sophisticated treatment of hybridization that allows for the existence of fractional, as well as integral, orbital contributions, and for hybridization indices greater than 3. The best way for these textbooks to build a bridge between their coverage of VSEPR theory and their coverage of VB theory is to teach both Rule 3 of the VSEPR model and Bent's rule for the hybrid orbital model, which explicitly links the *p*-character of a hybrid orbital to the electronegativity of the ligand and to the resulting bond angle. The additional link between the basicity or donor ability of a lone pair and the *s*-character of its hybrid orbital allows one to make yet further connections between these topics in the chapter on Brønsted acids and bases.

For a general chemistry class, it is suggested that the instructor provide the students with the conclusions of this paper and leave it at that. For a chemistry major and/or honors first-year chemistry class, it is suggested that the instructor actually provide the relevant derivations, as most honors students enjoy seeing how the conclusions were obtained. In addition, students can look up the bond angles and pK_a values for additional species.

Acknowledgments

Not applicable.

Authors contributions

All three authors contributed equally to all aspects of this publication.

Funding

The authors thank the Ralph E. Oesper Fund for financial support.

Competing interests

The authors declare that they have no known competing financial interests or personal relationships that could have appeared to influence the work reported in this paper.

Informed consent

Obtained.

Ethics approval

The Publication Ethics Committee of the Canadian Center of Science and Education.

The journal's policies adhere to the Core Practices established by the Committee on Publication Ethics (COPE).

Provenance and peer review

Not commissioned; externally double-blind peer reviewed.

Data availability statement

The data that support the findings of this study are available on request from the corresponding author. The data are not publicly available due to privacy or ethical restrictions.

Data sharing statement

No additional data are available.

References

Baldasare, C. A., & Seybold, P. G. (2020). Computational Estimation of the Gas-Phase and Aqueous Acidities of Carbon Acids. *J. Phys. Chem.*, *124,* 2152-2159. https://doi.org/10.1021/acs.jpca.9b11964

Bent, H. A. (1961). An Appraisal of Valence-Bond Structures and Hybridization in Compounds of the First-Row Elements. *Chem. Rev*., *61*, 235-275. https://doi.org/10.1021/cr60211a005

Bent, H. A. (1960). Distribution of Atomic s-Character in Molecules and Its Chemical Implications. *J. Chem. Educ*., *37*, 616-624. https://doi.org/10.1021/ed037p616

Brown, T. L., LeMay, H. E., Bursten, B. E., Murphy, C., Woodward, P., & Stoltzfus, M. (2022). *Chemistry, the Central Science*, 15th ed., Prentice Hall, Pearson Education: Upper Saddle River, NJ.

Brown, W. H., Iverson, B. L., Anslyn, E. V., & Foote, C. S. (2023). Organic Chemistry, 9th ed., Cengage: Boston, MA.

Gillespie, R. J. (1972). *Molecular Geometry,* Van Nostrand & Reinhold: London.

Gillespie, R. J., & Hargittai, I. (1991). *The VSEPR Model* of *Molecular Geometry*, Allyn and Bacon: Boston.

Gillespie, R. J., & Nyholm, R. S. (1957). Inorganic Stereochemistry. *Quart. Rev. Chem. Soc*., *11*, 339-380. https://doi.org/10.1039/qr9571100339

Gillespie, R. J., Humphreys, D. A., Colin Baird, N., & Robinson, E. A. (1986). *Chemistry*, Allyn & Bacon: Boston, MA.

Grushow, A., (2011). Is it Time to Retire the Hybrid Atomic Orbital?. *J. Chem. Educ*., *88*, 860-862. https://doi.org/10.1021/ed100155c

Holleman, A. F., & Wiberg, E. (2001). *Inorganic Chemistry*, Academic Press: New York, NY.

Hsu, C. Y., & Orchin, M. (1973). A Simple Method for Generating Sets of Orthonormal Hybrid Atomic Orbitals. *J. Chem. Educ.*, *50*, 114-118. https://doi.org/10.1021/ed050p114

Huheey, J. E., Keiter, E. A., & Keiter, R. L. (1993). *Inorganic Chemistr*y, 4th ed., Harper Collins, New York, NY, p. 222.

Karty, J. (2018). *Organic Chemistry*. 2nd ed., Norton: New York, NY.

Kepert, D. L. (1982). *Inorganic Stereochemistry*, Springer-Verlag: Berlin. https://doi.org/10.1007/978-3-642-68046-5

Klein, D. (2021). *Organic Chemistry,* 4th ed., Wiley: Hoboken, NJ.

Loudon, M., & Parise, J. (2021). *Organic Chemistry*, 7th ed., Macmillan: New York, NY.

MacKay, R. A., & Henderson, W. (2017). *Introduction to Inorganic Chemistry*, 6th ed., Blackie: Glasgow. https://doi.org/10.1201/9781315274676

March, J. (1992). *Advanced Organic Chemistry: Reactions, Mechanisms, and Structure,* 4th ed., Wiley-Interscience: New York, NY, and references cited therein.

Miessler, G. L. & Tarr, D. A. (2011). Inorganic Chemistry, 3rd ed., Pearson, Prentice Hall: Upper Saddle Roiver, NJ.

Molnar, J., Kolonits, M., & Hargittai, M. (1997). Molecular Structure of SbF_3 and BiF_3: an Electron Diffraction Study. *J. Mol. Struct.*, 413-414, 441-446. https://doi.org/10.1016/S0022-2860(97)00057-4

Moore, J. W., & Stanitski, C. L. (2015). *Chemistry, The Molecular Science*, 5th ed., Thomson, Brooks Cole: Belmont, CA.

Mullins, R. J. (2021). *Organic Chemistry*, Pearson: Hoboken, NJ.

Pauling, L. (1931). The Nature of the Chemical Bond: Application of Results Obtained from the Quantum Mechanics

and from a Theory of Paramagnetic Susceptibility to the Structure of Molecules. *J. Am. Chem. Soc., 53*, 1367-1400. https://doi.org/10.1021/ja01355a027

Pauling, L. (1960). *The Nature of the Chemical Bond*, 3rd ed., Cornell University Press: Ithaca, NY, 1960.

Silberberg, M. S., & Amateis, P. (2021) *Principles of General Chemistry*, 9th ed. McGraw-Hill Higher Education: New York, NY.

Slater, J. C. (1931). Directed Valence in Polyatomic Molecules. *Phys. Rev*., *37*, 481-489. https://doi.org/10.1103/PhysRev.37.481

Wade, L. G., & Simek, J. W. (2017). *Organic chemistry,* 9th ed., Pearson: Hoboken, NJ.

Weinhold, F. W., & Landis C. (2005). *Valency and Bonding: A Natural Orbital Donor-Acceptor Perspective*, Cambridge University Press: Cambridge, pp. 138-140.

Appendix

To illustrate the generality of the correlation between bond angles, converted to the fraction of *p*-character in the bonding hybrid orbitals, f_p, and the electronegativity differences between the bonded atoms, $\Delta EN = EN_X - EN_A$, in AX_3E and AX_2E_2 molecules, this appendix contains additional examples of this correlation. The bond angles of these compounds were obtained from calculated structures using the Gaussian suite of programs applying density functional theory, DFT, with B3LYP functionals and 6-311G++(d,2p) or the LANL 2DZ basis functions (Gaussian 16, Revision C.01). The calculated bond angles compared favorably with experimental bond angles when they were available. The electronegativities were taken from Pauling's electronegativity scale. The correlations are quite good ($R^2 > 0.95$, $R^2_{average} = 0.988$), especially considering that in many cases the electronegativity differences were down to 1 significant figure. Note that Table A2 and Figure A2 in the Appendix correspond to Table 3 and Figure 4 in the text, but with calculated rather than experimental bond angle data. Likewise, Table A5 and Figure A5 in the Appendix correspond to Table 2 and Figure 3 in the text, but with calculated rather than experimental bond angle data. Tables A1-A5 and Figures A1-A5 give correlations for AX_3E sequences in which either A or X are held constant; Tables A6-A10 and Figures A6-A10 do the same for sequences of AX_2E_2 molecules; and Tables A11-A12 and Figures A11-A12 give correlations for examples of AH_2X_2 molecules, where the lone pairs of electrons are replaced by bonded hydrogen atoms, and the angle of interest is the X-A-X angle.

AX_3E molecules

Table A1. Group 15 trihydrides: H_3N, PH_3, AsH_3, SbH_3.

Molecule: AX_3E	**NH_3**	**PH_3**	**AsH_3**	**SbH_3**
X-A-X angle (degrees) [a]	107.262	93.307	92.100	91.282
$\Delta EN = EN_X - EN_A$ [b]	-0.9	0.0	0.1	0.2
f_p (in the A-X bonds) [c]	0.771	0.945	0.965	0.978
f_s (in the A-X bonds) [c]	0.229	0.055	0.035	0.022
sp^i (in the A-X bonds) [c]	$sp^{3.37}$	$sp^{17.3}$	$sp^{27.3}$	$sp^{44.7}$
f_p (in the lone pair) [c]	0.687	0.164	0.106	0.066
f_s (in the lone pair) [c]	0.313	0.836	0.894	0.934

[a] Bond angles calculated by DFT: B3LYP 6-311G++(d,2p) or LANL 2DZ.

[b] Values of ΔEN calculated from Pauling electronegativities.

[c] Values of i, f_p, and f_s calculated from bond angles and equations 7, 8, and 9.

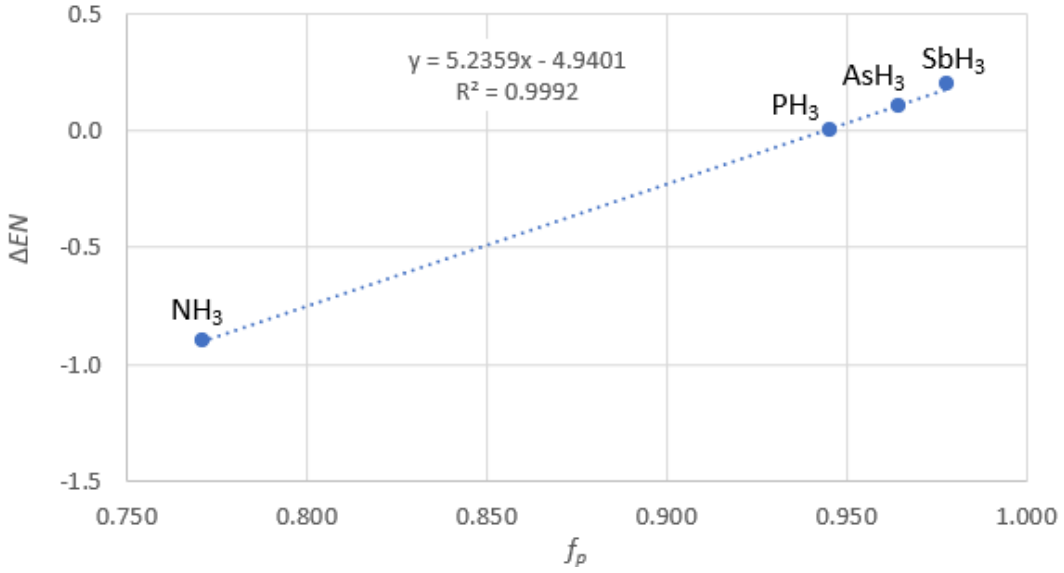

Figure A1. The linear correlation between ΔEN and f_p for the bonding orbitals of the Group 15 trihydrides

In this sequence the value of ΔEN for NH_3 is negative, indicating that the central atom is more electronegative than the ligand. In this case, the bonding pair is drawn closer to the central atom rather than to the ligand. This means, in turn, that the bond will exhibit an increase in its *s*-character rather than in its *p*-character resulting in an increase in the bond angle rather than in a decrease – exactly the opposite of the effect produced by a positive ΔEN value. We also encounter examples of this reversal in Figures A1, A2, A3, A6, A7, and A8 (where increasing the electronegativity of the *central* atom leads to a *decrease* in the *p*-character of the bonding orbitals).

Table A2. Group 15 trifluorides: NF_3, PF_3, AsF_3, SbF_3

Molecule: AX_3E	**NF_3**	**PF_3**	**AsF_3**	**SbF_3**
X-A-X angle (degrees) [a]	102.081	97.458	96.131	94.794
$\Delta EN = EN_X - EN_A$ [b]	1.0	1.9	2.0	2.1
f_p (in the A-X bonds) [c]	0.827	0.885	0.904	0.923
f_s (in the A-X bonds) [c]	0.173	0.115	0.096	0.077
sp^i (in the A-X bonds) [c]	$sp^{4.78}$	$sp^{7.70}$	$sp^{9.36}$	$sp^{11.97}$
f_p (in the lone pair) [c]	0.519	0.345	0.289	0.231
f_s (in the lone pair) [c]	0.481	0.655	0.711	0.769

[a] Bond angles calculated by DFT: B3LYP 6-311G++(d,2p) or LANL 2DZ.

[b] Values of ΔEN calculated from Pauling electronegativities.

[c] Values of i, f_p, and f_s calculated from bond angles and equations 7, 8 and 9.

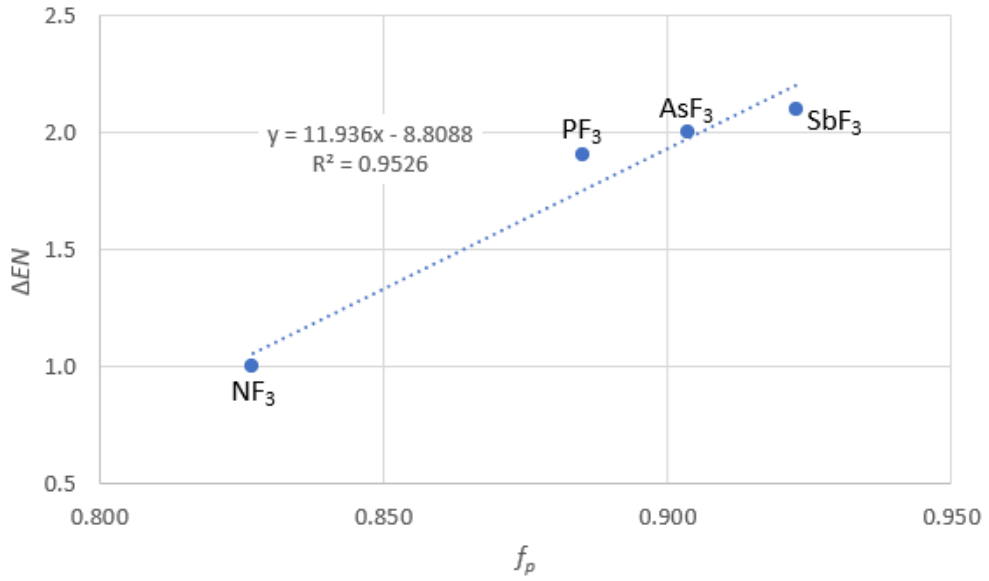

Figure A2. The linear correlation between ΔEN and f_p for the bonding orbitals of the Group 15 trifluorides.

Table A3. Group 15 trichlorides: NCl_3, PCl_3, $AsCl_3$, $SbCl_3$.

Molecule: AX_3E	**NCl_3**	**PCl_3**	**$AsCl_3$**	**$SbCl_3$**
X-A-X angle (degrees) [a]	108.248	101.041	99.675	98.386
$\Delta EN = EN_X - EN_A$ [b]	0.0	0.9	1.0	1.1
f_p (in the A-X bonds) [c]	0.762	0.839	0.856	0.873
f_s (in the A-X bonds) [c]	0.238	0.161	0.144	0.127
sp^i (in the A-X bonds) [c]	$sp^{3.19}$	$sp^{5.22}$	$sp^{5.95}$	$sp^{6.86}$
f_p (in the lone pair) [c]	0.715	0.482	0.432	0.382
f_s (in the lone pair) [c]	0.285	0.518	0.568	0.618

[a] Bond angles calculated by DFT: B3LYP 6-311G++(d,2p) or LANL 2DZ.

[b] Values of ΔEN calculated from Pauling electronegativities.

[c] Values of i, f_p, and f_s calculated from bond angles and equations 7, 8, and 9.

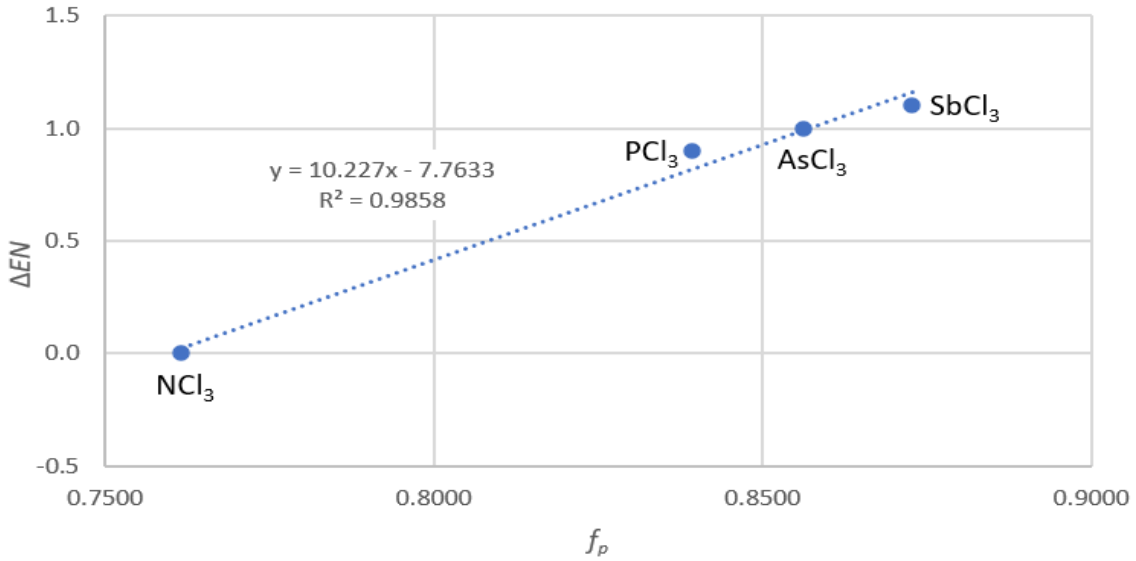

Figure A3. The linear correlation between ΔEN and f_p for the bonding orbitals of the Group 15 trihalides

Table A4. Nitrogen trihalides: NF_3, NCl_3, NBr_3, NI_3.

Molecule: AX_3E	**NF_3**	**NCl_3**	**NBr_3**	**NI_3**
X-A-X angle (degrees) [a]	102.081	108.248	109.092	111.711
$\Delta EN = EN_X - EN_A$ [b]	1.0	0.0	-0.2	-0.5
f_p (in the A-X bonds) [c]	0.827	0.762	0.754	0.730
f_s (in the A-X bonds) [c]	0.173	0.238	0.246	0.270
sp^i (in the A-X bonds) [c]	$sp^{4.78}$	$sp^{3.19}$	$sp^{3.06}$	$sp^{2.70}$
f_p (in the lone pair) [c]	0.519	0.715	0.739	0.810
f_s (in the lone pair) [c]	0.481	0.285	0.261	0.190

[a] Bond angles calculated by DFT: B3LYP 6-311G++(d,2p) or LANL 2DZ.

[b] Values of ΔEN calculated from Pauling electronegativities.

[c] Values of i, f_p, and f_s calculated from bond angles and equations 7, 8, and 9.

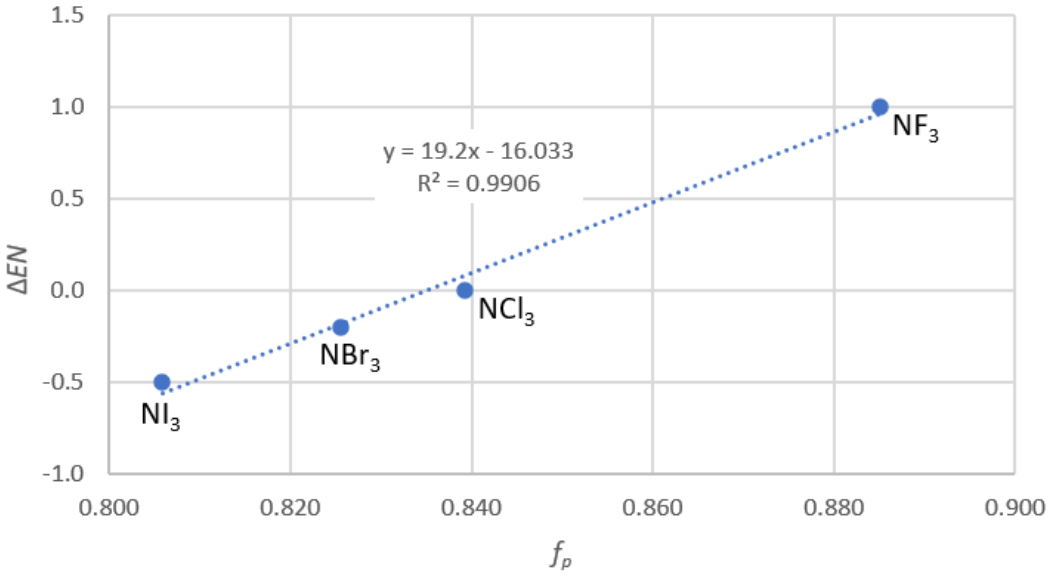

Figure A4. The linear correlation between ΔEN and f_p for the bonding orbitals of the nitrogen trihalides

Table A5. Phosphorus trihalides: PF_3, PCl_3, PBr_3, PI_3.

Molecule: AX_3E	**PF_3**	**PCl_3**	**PBr_3**	**PI_3**
X-A-X angle (degrees) [a]	97.458	101.041	102.203	103.939
$\Delta EN = EN_X - EN_A$ [b]	1.9	0.9	0.7	0.4
f_p (in the A-X bonds) [c]	0.885	0.839	0.826	0.806
f_s (in the A-X bonds) [c]	0.115	0.161	0.174	0.194
sp^i (in the A-X bonds) [c]	$sp^{7.70}$	$sp^{5.22}$	$sp^{4.73}$	$sp^{4.15}$
f_p (in the lone pair) [c]	0.345	0.482	0.523	0.582
f_s (in the lone pair) [c]	0.655	0.518	0.477	0.418

[a] Bond angles calculated by DFT: B3LYP 6-311G++(d,2p) or LANL 2DZ.

[b] Values of ΔEN calculated from Pauling electronegativities.

[c] Values of i, f_p, and f_s calculated from bond angles and equations 7, 8, and 9.

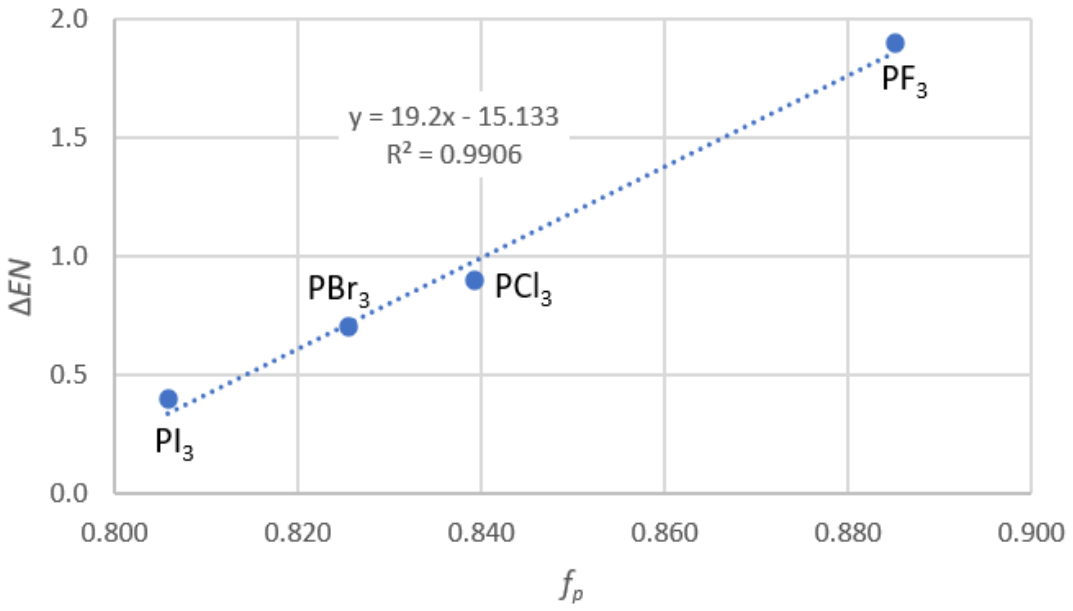

Figure A5. The linear correlation between ΔEN and f_p for the bonding orbitals of the phosphorus trihalides.

AX_2E_2 molecules

Table A6. Group 16 dihydrides: H_2O, H_2S, H_2Se, H_2Te

Molecule: AX_2E_2	**H_2O**	**H_2S**	**H_2Se**	**H_2Te**
X-A-X angle (degrees) [a]	104.897	92.276	91.083	90.315
$\Delta EN = EN_X - EN_A$ [b]	-1.4	-0.4	-0.3	0.0
f_p (in the A-X bonds) [c]	0.795	0.962	0.981	0.995
f_s (in the A-X bonds) [c]	0.205	0.038	0.019	0.005
sp^i (in the A-X bonds) [c]	$sp^{3.89}$	$sp^{25.2}$	$sp^{52.9}$	sp^{182}
f_p (in the lone pairs) [c]	0.705	0.538	0.519	0.505
f_s (in the lone pairs) [c]	0.295	0.462	0.481	0.495

[a] Bond angles calculated by DFT: B3LYP 6-311G++(d,2p) or LANL 2DZ.

[b] Values of ΔEN calculated from Pauling electronegativities.

[c] Values of i, f_p, and f_s calculated from bond angles and equations 7, 8, and 9.

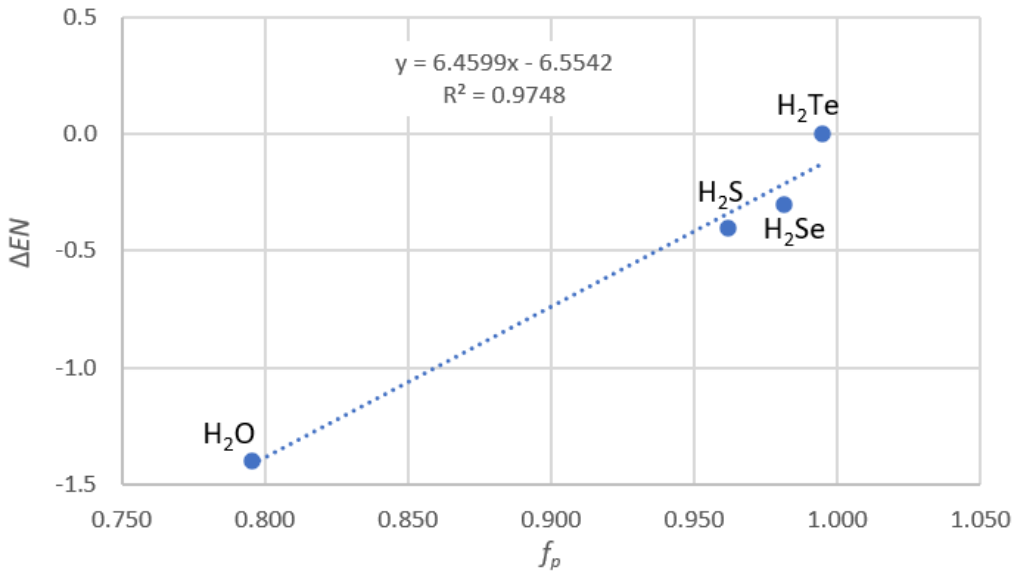

Figure A6. The linear correlation between ΔEN and f_p for the bonding orbitals of the Group 16 dihydrides.

Table A7. Group 16 difluorides: OF_2, SF_2, SeF_2, TeF_2.

Molecule: AX_2E_2	**OF_2**	**SF_2**	**SeF_2**	**TeF_2**
X-A-X angle (degrees) [a]	104.120	98.794	97.281	96.300
$\Delta EN = EN_X - EN_A$ [b]	0.5	1.5	1.6	1.9
f_p (in the A-X bonds) [c]	0.804	0.867	0.888	0.901
f_s (in the A-X bonds) [c]	0.196	0.133	0.112	0.099
sp^i (in the A-X bonds) [c]	$sp^{4.10}$	$sp^{6.54}$	$sp^{7.89}$	$sp^{9.11}$
f_p (in the lone pairs) [c]	0.696	0.633	0.612	0.599
f_s (in the lone pairs) [c]	0.304	0.367	0.388	0.401

[a] Bond angles calculated by DFT: B3LYP 6-311G++(d,2p) or LANL 2DZ.

[b] Values of ΔEN calculated from Pauling electronegativities.

[c] Values of i, f_p, and f_s calculated from bond angles and equations 7, 8, and 9.

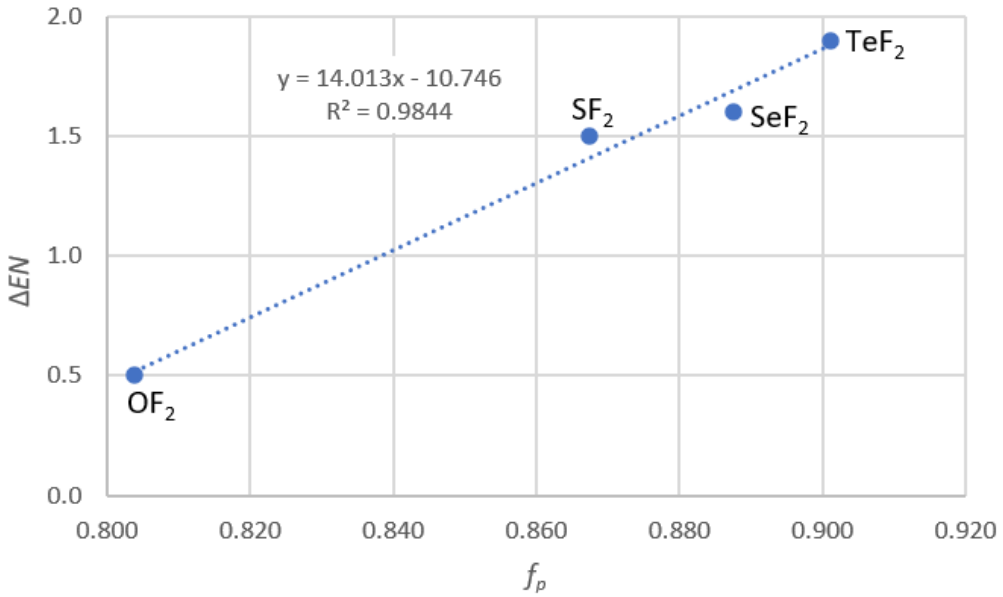

Figure A7. The linear correlation between ΔEN and f_p for the bonding orbitals of the Group 16 difluorides

Table A8. Group 16 dichlorides: OCl_2, SCl_2, $SeCl_2$, $TeCl_2$

Molecule: AX_2E_2	**OCl_2**	**SCl_2**	**$SeCl_2$**	**$TeCl_2$**
X-A-X angle (degrees) [a]	113.597	104.023	101.932	100.612
$\Delta EN = EN_X - EN_A$ [b]	-0.5	0.5	0.6	0.9
f_p (in the A-X bonds) [c]	0.714	0.805	0.829	0.844
f_s (in the A-X bonds) [c]	0.286	0.195	0.171	0.156
sp^i (in the A-X bonds) [c]	$sp^{2.50}$	$sp^{4.13}$	$sp^{4.84}$	$sp^{5.43}$
f_p (in the lone pairs) [c]	0.786	0.695	0.671	0.656
f_s (in the lone pairs) [c]	0.214	0.305	0.329	0.344

[a] Bond angles calculated by DFT: B3LYP 6-311G++(d,2p) or LANL 2DZ.

[b] Values of ΔEN calculated from Pauling electronegativities.

[c] Values of i, f_p, and f_s calculated from bond angles and equations 7, 8, and 9.

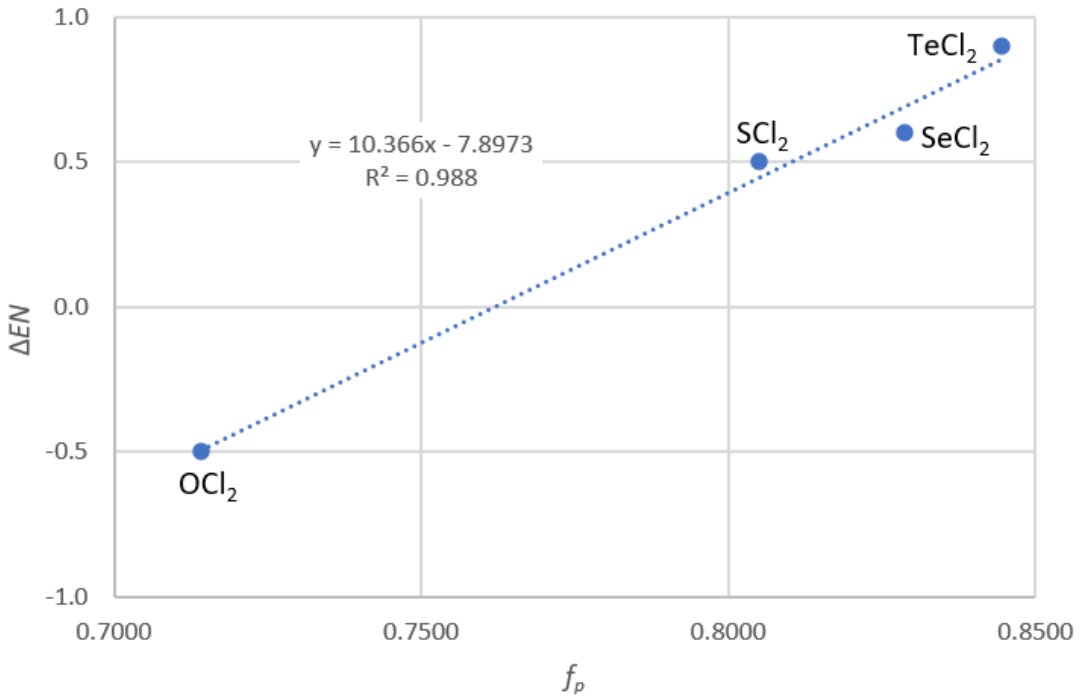

Figure A8. The linear correlation between ΔEN and f_p for the bonding orbitals of the Group 16 dichlorides

Table A9. Oxygen dihalides: F_2O, Cl_2O, Br_2O, I_2O.

Molecule: AX_2E_2	**F_2O**	**Cl_2O**	**Br_2O**	**I_2O**
X-A-X angle (degrees) [a]	104.120	113.597	115.474	120.418
$\Delta EN = EN_X - EN_A$ [b]	0.5	-0.5	-0.7	-1.0
f_p (in the A-X bonds) [c]	0.804	0.714	0.699	0.664
f_s (in the A-X bonds) [c]	0.196	0.286	0.301	0.336
sp^i (in the A-X bonds) [c]	$sp^{4.10}$	$sp^{2.50}$	$sp^{2.33}$	$sp^{1.98}$
f_p (in the lone pairs) [c]	0.696	0.786	0.801	0.836
f_s (in the lone pairs) [c]	0.304	0.214	0.199	0.164

[a] Bond angles calculated by DFT: B3LYP 6-311G++(d,2p) or LANL 2DZ.

[b] Values of ΔEN calculated from Pauling electronegativities.

[c] Values of i, f_p, and f_s calculated from bond angles and equations 7, 8, and 9.

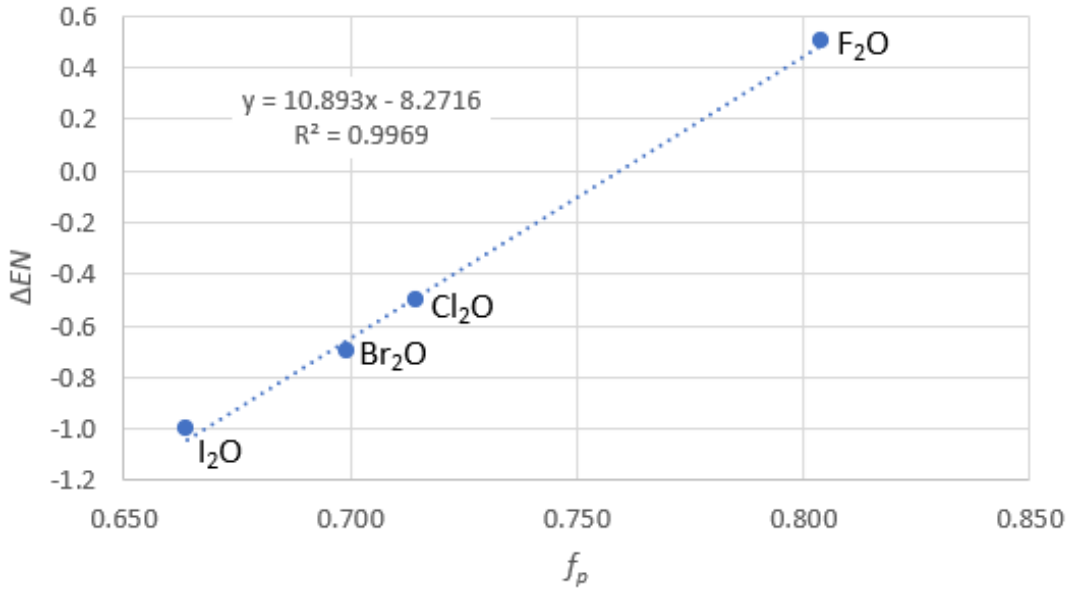

Figure A9. The linear correlation between ΔEN and f_p for the bonding orbitals of the oxygen dihalides

Table A10. Sulfur dihalides: SF_2, SCl_2, SBr_2, SI_2.

Molecule: AX_2E_2	**SF_2**	**SCl_2**	**SBr_2**	**SI_2**
X-A-X angle (degrees) [a]	98.794	104.023	105.628	107.644
$\Delta EN = EN_X - EN_A$ [b]	1.5	0.5	0.3	0.0
f_p (in the A-X bonds) [c]	0.867	0.805	0.788	0.767
f_s (in the A-X bonds) [c]	0.133	0.195	0.212	0.233
sp^i (in the A-X bonds) [c]	$sp^{6.54}$	$sp^{4.13}$	$sp^{3.71}$	$sp^{3.30}$
f_p (in the lone pairs) [c]	0.633	0.695	0.712	0.733
f_s (in the lone pairs) [c]	0.367	0.305	0.288	0.267

[a] Bond angles calculated by DFT: B3LYP 6-311G++(d,2p) or LANL 2DZ.

[b] Values of ΔEN calculated from Pauling electronegativities.

[c] Values of i, f_p, and f_s calculated from bond angles and equations 7, 8, and 9.

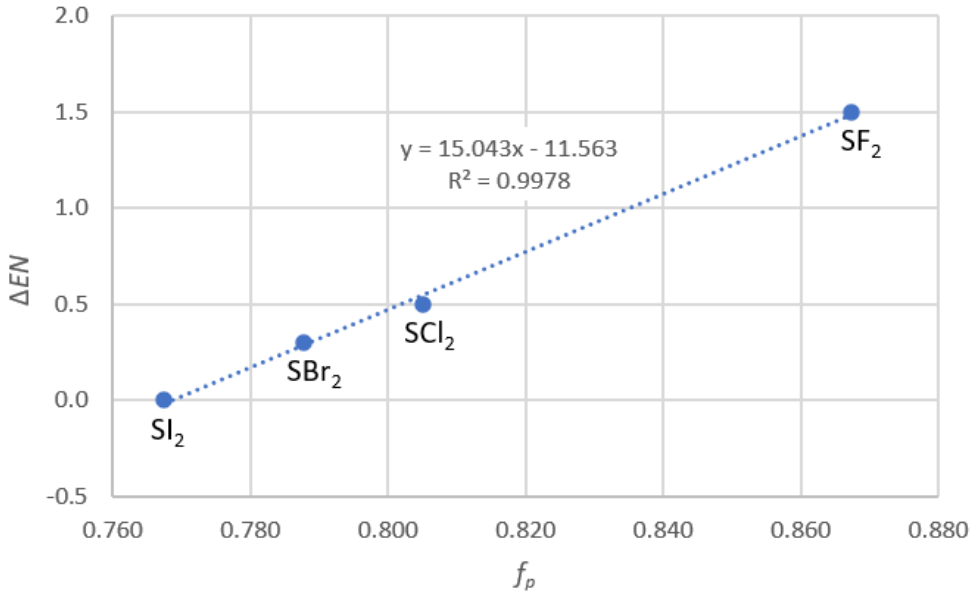

Figure A10. The linear correlation between ΔEN and f_p for the bonding orbitals of the sulfur dihalides

AH_2X_2 molecules

Table A11. Dihalomethanes: CH_2F_2, CH_2Cl_2, CH_2Br_2, CH_2I_2.

Molecule: CH_2X_2	**CH_2F_2**	**CH_2Cl_2**	**CH_2Br_2**	**CH_2I_2**
X-A-X angle (degrees) [a]	108.435	113.173	114.392	116.246
$\Delta EN = EN_X - EN_A$ [b]	1.5	0.5	0.3	0.0
f_p (in the A-X bonds) [c]	0.760	0.718	0.708	0.693
f_s (in the A-X bonds) [c]	0.240	0.282	0.292	0.307
sp^i (in the A-X bonds) [c]	$sp^{3.16}$	$sp^{2.54}$	$sp^{2.42}$	$sp^{2.26}$
f_p (in the A-H bonds) [c]	0.740	0.782	0.792	0.807
f_s (in the A-H bonds) [c]	0.260	0.218	0.208	0.193

[a] Bond angles calculated by DFT: B3LYP 6-311G++(d,2p) or LANL 2DZ.

[b] Values of ΔEN calculated from Pauling electronegativities.

[c] Values of i, f_p, and f_s calculated from bond angles and equations 7, 8, and 9.

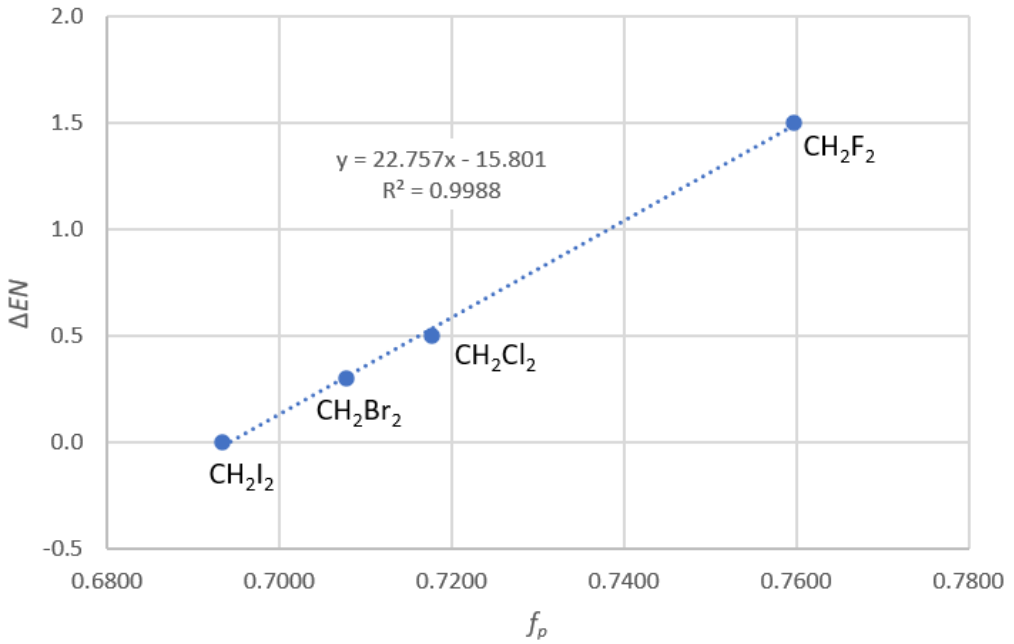

Figure A11. The linear correlation between ΔEN and f_p for the A-X bonding orbitals of the dihalomethanes

Table A12. Dihalosilanes: SiH_2F_2, SiH_2Cl_2, SiH_2Br_2, SiH_2I_2

Molecule: SiH_2X_2	**SiH_2F_2**	**SiH_2Cl_2**	**SiH_2Br_2**	**SiH_2I_2**
X-A-X angle (degrees) [a]	107.638	110.431	111.497	112.437
$\Delta EN = EN_X - EN_A$ [b]	2.2	1.2	1.0	0.7
f_p (in the A-X bonds) [c]	0.767	0.741	0.732	0.724
f_s (in the A-X bonds) [c]	0.233	0.259	0.268	0.276
sp^i (in the A-X bonds) [c]	$sp^{3.30}$	$sp^{2.86}$	$sp^{2.73}$	$sp^{2.62}$
f_p (in the A-H bonds) [c]	0.733	0.759	0.768	0.776
f_s (in the A-H bonds) [c]	0.267	0.241	0.232	0.224

[a] Bond angles calculated by DFT: B3LYP 6-311G++(d,2p) or LANL 2DZ.

[b] Values of ΔEN calculated from Pauling electronegativities.

[c] Values of i, f_p, and f_s calculated from bond angles and equations 7, 8, and 9.

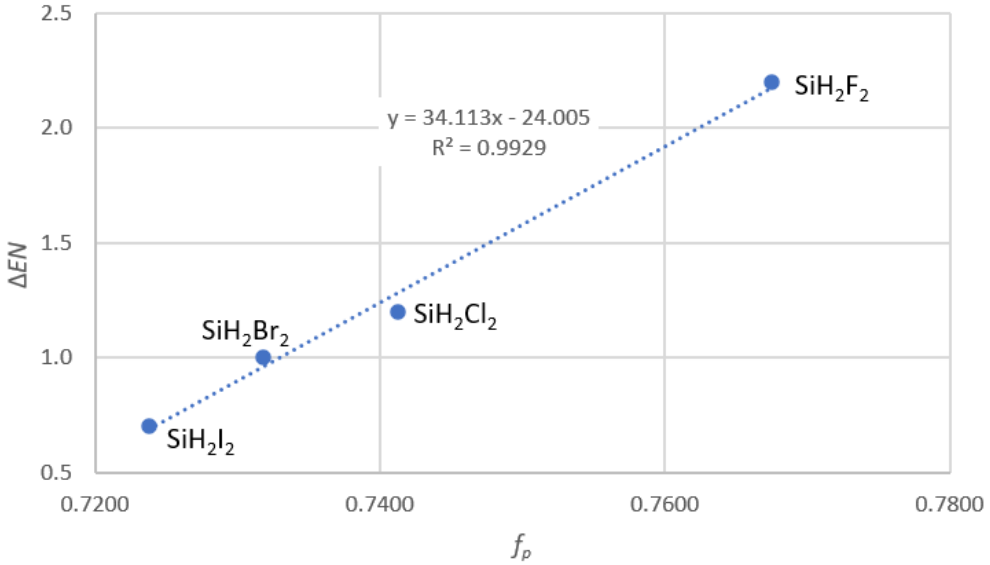

Figure A12. The linear correlation between ΔEN and f_p for the A-X bonding orbitals of the dihalosilanes

Appendix Reference

Gaussian 16, Revision C.01: Frisch, M.J., Trucks, G. W., Schlegel, H. B., Scuseria, G. E., Robb, M. A., Cheeseman, J. R., Scalmani, G., Barone, V., Petersson, G. A., Nakatsuji, H., Li, X., Caricato, M., Marenich, A. V., Bloino, J., Janesko, B. G., Gomperts, R., Mennucci, B., Hratchian, H. P., Ortiz, J. V., Izmaylov, A. F., Sonnenberg, J. L., Williams-Young, D., Ding, F., Lipparini, F., Egidi, F., Goings, J., Peng, B., Petrone, A., Henderson, T., Ranasinghe, D., Zakrzewski, V. G., Gao, J., Rega, N., Zheng, G., Liang, W., Hada, M., Ehara, M., Toyota, K., Fukuda, R., Hasegawa, J., Ishida, M., Nakajima, T., Honda, Y., Kitao, O., Nakai, H., Vreven, T., Throssell, K., Montgomery, J. A., Peralta, J. E., Ogliaro, F., Bearpark, M. J., Heyd, J. J., Brothers, E. N., Kudin, K. N., Staroverov, V. N., Keith, T. A., Kobayashi, R., Normand, J., Raghavachari, K., Rendell, A. P., Burant, J. C., Iyengar, S. S., Tomasi, J., Cossi, M., Millam, J. M., Klene, M., Adamo, C., Cammi, R., Ochterski, J. W., Martin, R. L, Morokuma, K., Farkas, O., Foresman, J. B., Fox, D. J. Gaussian, Inc., Wallingford CT, 2019